Absorption of a Polyelectrolyte Brush into an Oppositely Charged Layer

E. B. Zhulina*,†,§ and O. V. Borisov‡,§

Department of Chemical, Engineering, University of Pittsburgh, Pittsburgh, Pennsylvania 15261, Department of Physical and Colloid Chemistry, University of Wageningen, 6703 HB Wageningen, The Netherlands, and Institute of Macromolecular Compounds, Russian Academy of Sciences, 199004, St. Petersburg, Russia

Received May 28, 1998; Revised Manuscript Received August 13, 1998

ABSTRACT: We have developed an analytical theory which describes the equilibrium structure of a polyelectrolyte brush interacting with oppositely charged sublayer. We consider sparsely grafted polyions with quenched charges that are immersed in a salt-free solution and form a brush of thickness H. An oppositely charged sublayer of thickness R is located near the grafting surface. We analyze the cases of partial ($H > R$) and total ($H < R$) absorption of polyions into the sublayer. We demonstrate that for partially absorbed polyions ($H > R$), the brush thickness H is not sensitive to a particular shape and range of charge distribution in sublayer but is determined by the total amount of charge immobilized in sublayer. Our findings indicate that, in a partially absorbed system, the brush undergoes an internal segregation. That is, part of the polyions are totally embedded into the sublayer, while the rest of the chains still form a brush. When the brush is totally absorbed into the sublayer ($H < R$), the structure of the brush depends on the particular shape of distribution of the immobilized opposite charge.

1. Introduction

Conformations of flexible polyelectrolytes tethered at solid−liquid interfaces were extensively investigated theoretically during the past decade.[1−14] The experimental studies of tethered polyelectrolytes are less evolved. However, recent experimental observations[15−18] indicate reasonable agreement with the basic theoretical picture.

The importance of understanding the static and dynamic properties of tethered polyelectrolytes is related to their broad application for stabilization of colloid dispersions in aqueous media.[19] Besides traditional industries employing stabilization and flocculation of colloids (that is, papermaking, paints, food, cosmetics, etc.), many biomedical systems are also relevant. For example, decoration by polymers of liposome-based drug-delivery systems, makes those systems resistant against lymphocytes.[20] Protection of blood cells (erythrocytes) against virus of influenza can be also enhanced by polymer coatings.[21]

From a theoretical point of view, the basic features of polyelectrolyte brushes are determined by Coulomb interactions between the charges on the chains. The long-range character of electrostatic forces makes polyelectrolyte brushes more sophisticated systems than their neutral counterparts. The presence of charges on the tethered chains manifests itself in more extended and stable coatings. Interactions between such coatings can be mediated not only by varying the length and the grafting density of the tethered chains but also by such additional factors as the amount of ionized groups on the chains, the ionic strength of the solution, and pH. These new opportunities make polyelectrolyte brushes an attractive object for both theory and experiment.

Up to now, theoretical studies on polyelectrolyte brushes involved mostly neutral, inert grafting surfaces. However, in many realistic systems, the solid−liquid interfaces are charged. For example, in the case of silica immersed in water, surface charge appears due to ionization of surface functional groups and the charge is localized in a narrow presurface layer. Surface charge also appears due to the adsorption of ionic surfactants at water−air interfaces. In a more complex system of polyelectrolytes adsorbing at a solid−liquid interface, the interface bears a spatially distributed charge.[22] This charge is associated mainly with the loops formed by adsorbed polyelectrolytes. Here, the width of such a charge distribution is governed by the thickness of the adsorbed layer. The spatially distributed charges can be created also by adhesion of thin films of polyelectrolyte gels to the grafting surface, etc. In all those cases, an interface comprises a charged layer of considerable thickness.

The goal of this work is to investigate how interaction between a brush which is composed of long flexible polyelectrolytes and an oppositely charged presurface sublayer affects the structure and properties of the brush. In our previous paper,[14] we have developed an analytical self-consistent field theory which allowed us to examine in detail the equilibrium properties of polyelectrolyte brushes tethered onto neutral surfaces. We now extend our theory for the case when the grafting surface bears an oppositely charged sublayer. In this paper we consider only a salt-free solution (that is, the system where the polyelectrolyte effects are most pronounced), while in our subsequent work we will focus at the effect of a low molecular weight salt which screens electrostatic interactions between the polyions.

As we demonstrate below, an attraction between a brush and an oppositely charged thin sublayer can dramatically affect the structure of the system. As a result of such interaction, the brush undergoes an internal segregation. Part of the chains are totally embedded into the sublayer and shield its charge, while the rest still form a brush which protrudes far in solution. The central result of this paper is that a segregated polyelectrolyte brush is characterized by certain "universality". Namely, the electrostatic poten-

† University of Pittsburgh.
‡ University of Wageningen.
§ Russian Academy of Sciences.

10.1021/ma980845j CCC: $15.00
Published on Web 09/25/1998

tial and the overall thickness of such a brush are not sensitive to a particular shape and range of charge distribution in the sublayer, but are determined only by the total amount of the sublayer charge.

The rest of the paper is organized as follows. In section II we describe our model. In section III we present the mathematical formalism and obtain the major relationships for the characteristics of the system. In section IV we discuss the results, while in section V we summarize our conclusions.

2. Model

We consider a brush composed of long polyelectrolyte chains. The chains are irreversibly grafted onto a planar surface with the grafting density $1/s$ (s is area per chain) and are immersed into a polar solvent (water). We let N be the total number of units in a chain and α be the fraction of the charged monomer units in a polyion. (We choose a symmetrical segment of the chain of size a as a unit.)

The total charge of such a polyion is given by $Q_0 = \alpha N$ and each chain provides Q_0 monovalent counterions into the bulk solution. We assume that the chains are flexible (i.e., the length of the Kuhn segment A is on the order of unit size a) and that the Bjerrum length l_B is on the order of a as well. That is, $l_B = e^2/\epsilon k_B T \cong a$ where ϵ is the dielectric constant of the solvent and e is the elementary charge. We assume also that the charges on the chains are quenched (i.e., $\alpha = \text{const}$) and that the polyions are charged rather weakly, $\alpha \ll 1$. Due to the condition $\alpha \ll 1$ and the intrinsic flexibility of the chains ($A = a$), the direct repulsions between the neighboring charges do not change the persistence length[23] and the local statistics in the chain remains essentially Gaussian. However, due to the long-range nature of the electrostatic interactions, the interchain repulsions lead to the strong stretching of the chains normally to the surface. We assume that in this brush regime the interactions between the charged monomers dominate over the short-range nonelectrostatic interactions between the uncharged monomers. In our further analysis we neglect the contribution due to the latter, nonelectrostatic interactions and focus on the effect of the dominant, electrostatic forces on the brush structure.

We assume that the grafting surface bears a sublayer of a fixed width R that is charged oppositely to the polyions. We let the chains be charged positively and the layer be charged negatively. The charge is distributed with the density $\rho_s(x)$ where x is the distance from the surface. The total charge of the layer per tethered chain is given by $Q = s\int_0^R \rho_s(x)\,dx$. (For a specific case of a uniformly charged layer, $\rho_s(x) = \rho_s$ and $Q = sR\rho_s$.) We introduce the ratio $\gamma = Q/Q_0$ as a dimensionless measure of the sublayer charge.

The solution contains mobile ions which, together with the charged sublayer, compensate the charge on the tethered polyions. (The overall system, brush + sublayer + solution, is electroneutral as a whole.) Due to the gradients in charge distribution in the direction x normal to the surface, the mobile ions are spread nonuniformly along the x direction, while in the two other directions, y and z, the ion distribution is smeared out. We thus introduce the concentration of the counterions as $\rho(x)$ which depends only on the distance x from the grafting surface. The spatial distribution of the ions is related to the corresponding electrostatic potential, $\psi(x)$, via the Boltzmann law. Namely

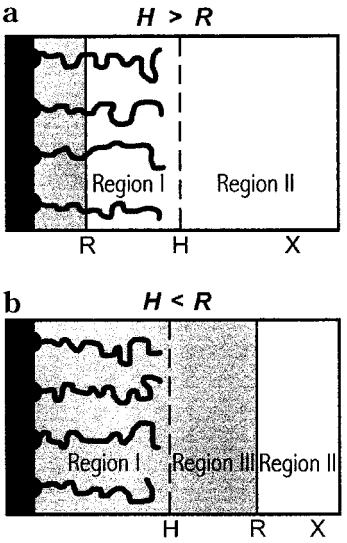

Figure 1. Schematic of a polyelectrolyte brush and an oppositely charged sublayer (shaded). The polymer is distributed in the range $0 < x < H$ (region I); the sublayer charge is localized in the range $0 < x < R$ (that is within region I in case of thin layers (a) and within regions I and III in case of thick layers (b)). Mobile ions are distributed in all three regions, I, II, and III.

$$\rho(x) = \rho(H)e^{e\psi(x)/k_B T} = \rho(H)e^{\Psi(x)} \qquad (1)$$

where $\rho(H)$ is the concentration of the ions at the edge of the brush, $x = H$, and $\Psi(x) = e\psi(x)/k_B T$ is the reduced electrostatic potential. We thus set the electrostatic potential to be zero at the boundary between the brush and the solution, $\Psi(H) = 0$. Due to a finite number of the counterions per chain, their concentration at an infinite distance from the surface, $x = \infty$, should be equal to zero. Thus, we have another boundary condition for the electrostatic potential, $\Psi(\infty) = -\infty$.

Figure 1 depicts schematically the system under consideration. The tethered polyions distribute their units in a layer of finite thickness H. The oppositely charged sublayer of thickness R can be totally embedded into the body of the brush (the case of a "thin layer" in Figure 1a), or protrude outside of the brush (the case of a "thick layer" in Figure 1b). The brush contains also the mobile counterions. At distances $x > H$, the concentration of polymer units equals zero. Here, only the counterions and the immobilized charge of the sublayer (as in Figure 1b) contribute to the local charge density in the solution. Below we present the mathematical formalism that enables us to obtain the equilibrium characteristics of the system (i.e., the spatial distributions of the mobile ions and polymer segments, brush thickness, etc.) at various dimensions of the charged sublayer R and the charge densities $\rho_s(x)$.

3. General Formalism

We consider the cases $H > R$ and $H < R$ separately. We distinguish these two situations as a partial and a total absorption of the tethered polyions into the sublayer. We start with the case of partial absorption, i.e., the case $H > R$.

3.1. Partial Absorption. Our analysis is based on direct solutions of the Poisson−Boltzmann equations for charge distributions inside and outside the brush. We

denote the regions located at $0 < x < H$ and at $x > H$ as regions I and II, respectively (see Figure 1a). We have

$$\Delta\Psi_1(x) = -4\pi l_B[\alpha c(x) - \rho(H)e^{\Psi_1(x)} - \rho_s(x)] \quad (2)$$

$$\Delta\Psi_2(x) = 4\pi l_B \rho(H) e^{\Psi_2(x)} \quad (3)$$

Here, $\Psi(x) = e\psi(x)/k_BT$ is the dimensionless electrostatic potential created by the charges on the chains and in the sublayer as well as by the mobile ions (indexes 1 and 2 indicate regions I and II, respectively), and $c(x)$ is the concentration of polymer units at distance x from the surface. The first term in brackets on the right side of eq 3 describes the profile of the immobilized charge on the chains, the second accounts for the counterions, while the last term is due to the charged presurface layer. Since there is no polymer in region II, and the charged sublayer is completely localized in region I, the right side of the Poisson−Boltzmann equation for region II (that is, eq 3), contains the contribution only due to the mobile counterions.

We focus on the case where the tethered polyions are strongly stretched with respect to their Gaussian size. The strong stretching limit ensures a specific form of the chemical potential μ/k_BT of a polymer unit in the brush which is formed by the chains with Gaussian elasticity. The form of this potential is parabolic[24]

$$\mu(x)/k_BT = \text{constant} - 3\pi^2x^2/8a^2N^2 \quad (4)$$

where an indefinite *constant* depends on the external conditions. In the absence of the nonelectrostatic interactions, the only contribution to the chemical potential μ is due to the electrostatic field in the brush. Correspondingly, in the strong stretching limit, the electrostatic potential inside the brush (i.e., in region I) should be parabolic. More specifically, the normalized electrostatic potential $\Psi_1(x)$ can be represented as[14]

$$\Psi_1(x) = \Psi_1(0) - x^2/H_0^2 \quad (5)$$

where

$$H_0 = a(8/3\pi^2)^{1/2}\alpha^{1/2}N \quad (6)$$

is a certain characteristic length scale (we will discuss its physical meaning later) and $\Psi_1(0)$ is the value of the electrostatic potential at the grafting surface. Since we choose Ψ_1 to be zero at $x=H$, we have

$$\Psi_1(0) = H^2/H_0^2 \quad (7)$$

While a detailed derivation of eq 5 can be found in ref 14, the transition from eq 4 to eq 5 can be explained by a simple argument. Since only a fraction α of all the polymer units is charged, an effective potential acting at any unit located at distance x, is just $\mu(x) = \alpha\Psi_1(x)$. By substituting the above expression for μ into eq 4, we immediately arrive at eqs 5 and 6.

By substituting the expression for $\Psi_1(x)$ from eq 5 into eq 2, we get a relationship between the density profiles of the ions and of the polymer

$$\alpha c(x) = \rho_s(x) + \rho(H)e^{\Psi_1(x)} + \frac{1}{2\pi l_B H_0^2} \quad (8)$$

We now apply the condition that the total number of polymer units inside the brush is conserved, to find

$$\int_0^H c(x)\,dx = Na^3/s \quad (9)$$

By substituting eq 8 into eq 9 and using eq 5 we have

$$\frac{\alpha N - Q_0}{s} = \frac{H}{2\pi l_B H_0^2} + \rho(H)e^{H^2/H_0^2}\int_0^H e^{-x^2/H_0^2}\,dx \quad (10)$$

We now introduce reduced variables. Namely, the reduced thickness of the brush

$$h = H/H_0 \quad (11)$$

and the parameter k which is proportional to the concentration of the counterions at the edge of the brush

$$k = 2\pi l_B H_0^2 \rho(H) \quad (12)$$

We introduce also the Gouy−Chapmann screening length[25]

$$\Lambda = \frac{s}{2\pi l_B \alpha N} \quad (13)$$

which determines the decay of the counterion cloud near a charged surface with bare surface charge density Q_0/s.

In the reduced variables, eq 10 reads

$$(1 - \gamma)\zeta = h + ke^{h^2}\int_0^h e^{-t^2}\,dt \quad (14)$$

where $\zeta = H_0/\Lambda$.

Equation 14 contains two unknown variables, h and k. To find an additional relationship between h and k, we have to solve the Poisson−Boltzmann equation in region II (cf., eq 3). We employ a routine scheme to solve eq 3. Namely, we introduce the new variable

$$p_2(\Psi_2) = \frac{d\Psi_2}{dx} \quad (15)$$

Then, eq 3 is reduced to a differential equation of the first order with respect to p_2, that reads as

$$\frac{d(p_2^2)}{d\Psi_2} = 8\pi l_B \rho(H) e^{\Psi_2} \quad (16)$$

After substituting the variable k and performing the first integration with respect to Ψ_2, we have

$$p_2^2 = \frac{4k}{H_0^2}e^{\Psi_2} + C_1 \quad (17)$$

where C_1 is an indefinite constant. We calculate C_1 by employing the condition of the electroneutrality of our system. That is, the strength of the electric field at infinite distance from the surface should be equal to zero, $p_2(\infty) = 0$. As a result, we obtain $C_1 = 0$ and

$$p_2 = \frac{d\Psi_2}{dx} = -\frac{2(k)^{1/2}}{H_0}e^{\Psi_2/2} \quad (18)$$

We now use the fact that both the electrostatic potential Ψ and its derivative $d\Psi/dx$ should be continuous at the

boundary between the two regions, I and II (i.e., at the edge of the brush $x = H$). Namely

$$\Psi_1(H) = \Psi_2(H) = 0 \tag{19}$$

and

$$\left(\frac{d\Psi_1}{dx}\right)_{x=H} = \left(\frac{d\Psi_2}{dx}\right)_{x=H} = -\frac{2h}{H_0} \tag{20}$$

The latter condition gives with the account of eqs 19 and 18 the relationship between h and k

$$h^2 = k \tag{21}$$

By performing the second integration of eq 18, we find the dependence of the electrostatic potential Ψ_2 on the reduced distance $\xi = x/H_0$ as

$$\Psi_2(\xi) = -2\ln[(\xi - h + 1/h)h] \tag{22}$$

By substituting eq 21 into eq 14, we arrive at the final equation for the brush thickness h

$$(1-\gamma)\zeta = h + h^2 e^{h^2}\int_0^h e^{-t^2}\,dt \tag{23}$$

Equation 23 determines the dependence of the brush thickness $h = H/H_0$ on the magnitude of charge in the presurface sublayer, γ, and on the ratio $\zeta = H_0/\Lambda$. At $\gamma = 0$, i.e., when there is no charge in the sublayer, eq 23 reduces to the equation, eq 53, obtained in ref 14. As discussed in ref 14, the value of ζ determines the distribution of the counterions. At values of $\zeta \ll 1$, the attraction of the ions to the brush is weak with respect to their thermal energy, and the ions are spread far above the edge of the brush. The characteristic scale of this distribution is the Gouy−Chapmann length Λ. The brush is nearly barely charged and we refer to this regime as the unscreened regime of a polyelectrolyte brush. On the other hand, when $\zeta \gg 1$, a strong attraction between the ions and the polyions pushes the ions to "condense" into the brush and screen the repulsions between the polyions. Here, the brush is almost electroneutral and is swollen by the osmotic pressure of the trapped counterions. We refer to this regime as the "osmotic" regime of a polyelectrolyte brush. The characteristic scale of the ion distribution in this limit is given by H_0. Thus, parameter ζ can be envisioned as the ratio of the two screening lengths, H_0 and Λ.

An increase in γ leads to a monotonic decrease in brush thickness h. A spectacular feature of eq 23 is, however, that the overall thickness h of the polyelectrolyte brush depends only on the total amount of the immobilized charge in the layer (through the value of γ) but not on the particular shape and range of the charge distribution, $\rho_s(x)$. We shall discuss this in more detail below, in the Discussion.

Provided that h is known, one can calculate the profiles of polymer units and of the mobile ions inside and outside the brush. Namely, the profile of ions inside the brush, $\rho_1(x)$, has the Gaussian shape and is given by

$$\rho_1(\xi) = \frac{h^2}{2\pi l_B H_0^2} e^{h^2-\xi^2} = \rho_0 h^2 \zeta^{-1} e^{h^2-\xi^2} \tag{24}$$

while the profile of ions outside of the brush yields

$$\rho_2(\xi) = \frac{h^2}{2\pi l_B H_0^2}\frac{1}{(\xi - h + 1/h)^2} = \rho_0\frac{1}{\zeta(\xi - h + 1/h)^2} \tag{25}$$

Here, $\rho_0 = \alpha N a^3/sH_0$ is the characteristic density of the counterions and $\xi = x/H_0$ is the reduced distance from the surface. The profile of polymer units is determined by eqs 8, 5 and 7 to give

$$\alpha c(\xi) = \rho_s(\xi) + \frac{h^2}{2\pi l_B H_0^2} e^{h^2-\xi^2} + \frac{1}{2\pi\, l_B H_0^2} \tag{26}$$

It is remarkable that the overall charge density (comprising the contributions due to the charged monomers, the counterions, and the immobilized charge in sublayer) is constant throughout the brush to provide the parabolic profile of the electrostatic potential.

The strong stretching limit, which we consider in this paper, ensures not only the parabolic shape of the electrostatic potential in the brush but also the interconnection between the distribution function of the free ends of the tethered chains, $g(x)$, and the profile of polymer units, $c(x)$.[24] Namely

$$c(x) = \frac{2Na^3}{\pi s}\int_x^H \frac{g(x')\,dx'}{\sqrt{x'^2 - x^2}} \tag{27}$$

A more detailed discussion of the above relationship can be found in the original papers on the strong stretching limit, see for example ref 24. By solving eq 27 as the integral equation with respect to $g(x)$ for a given functional form of $\rho_s(x)$ (see ref 14 for details), we can obtain the analytical expression for the distribution of the free ends. In particular, for a uniformly charged sublayer, $\rho_s(x) = \rho_s$, we get two expressions for $g(x)$, one for $x < R$ and another for $x > R$. Namely

$$g(\xi)H_0 = \xi\left[\zeta^{-1}\left(\frac{1+h^2}{\sqrt{h^2-\xi^2}} + 2h^2 e^{h^2-\xi^2}\int_0^{\sqrt{h^2-\xi^2}} e^{-t'^2}\,dt'\right) + \gamma\frac{1}{r\sqrt{r^2-\xi^2}}\right] \tag{28}$$

when $\xi < r$ and

$$g(\xi)H_0 = \xi\zeta^{-1}\left(\frac{1+h^2}{\sqrt{h^2-\xi^2}} + 2h^2 e^{h^2-\xi^2}\int_0^{\sqrt{h^2-\xi^2}} e^{-t'^2}\,dt'\right)$$

when $\xi > r$. Here, $r = R/H_0$ is the reduced thickness of the charged sublayer.

3.2. Total Absorption of Polyions. We now shift our attention to the case when $H < R$. For such a system, we will consider just a particular case that the charge in the sublayer is distributed uniformly, i.e., $\rho_s(x) = \rho_s$. Here, we distinguish three regions (see Figure 1b). Namely, the range $0 < x < H$ is again denoted as region I; the range $R < x$ is referred to as region II, while the intermediate region III covers the range $H < x < R$. In the latter region, the concentration of polymer is zero but the charge density in the sublayer is still given by ρ_s. As before, we focus on the solution of the Poisson−Boltzmann equations in these regions.

We have, correspondingly

$$\Delta\Psi_1(x) = -4\pi l_B[\alpha c(x) - \rho(H)e^{\Psi_1(x)} - \rho_s] \quad (29)$$

$$\Delta\Psi_2(x) = 4\pi l_B \rho(H) e^{\Psi_2(x)} \quad (30)$$

and

$$\Delta\Psi_3(x) = 4\pi l_B[\rho_s + \rho(H)e^{\Psi_3(x)}] \quad (31)$$

We introduce now an additional reduced variable

$$\omega = 2\pi l_B H_0^2 \rho_s = \frac{\gamma\zeta}{r} \quad (32)$$

where as before, $\zeta = H_0/\Lambda$ and $r = R/H_0$. Since the electrostatic potential in region I (i.e., inside the brush) is parabolic and is given by eq 5, by substituting eq 5 into eq 29, we obtain the expression for the polymer profile

$$\alpha c(x) = \rho_s + \rho(H)e^{(H^2-x^2)/H_0^2} + \frac{1}{2\pi l_B H_0^2} \quad (33)$$

By normalizing the polymer profile according to eq 9, we arrive at the expression for the reduced brush thickness h that reads

$$\zeta = h(1+\omega) + ke^{h^2}\int_0^h e^{-t^2}\,dt \quad (34)$$

To find another relationship between h and k, we solve the Poisson−Boltzmann equations in regions II and III (i.e., eqs 30 and 31). We again employ the routine scheme which is described in the previous subsection and obtain

$$p_2 = \frac{d\Psi_2}{dx} = -2\frac{\sqrt{k}}{H_0}e^{\Psi_2/2} \quad (35)$$

$$p_3 = \frac{d\Psi_3}{dx} = -\frac{2}{H_0}\sqrt{\omega\Psi_3 + ke^{\Psi_3} + h^2 - k} \quad (36)$$

We note that the indefinite constant due to the first integration of eq 31 was calculated from the condition 20. We now employ the condition of continuity of the field strength at the second boundary, $x = R$. Namely, $p_2(x = R) = p_3(x = R)$. As a result, we obtain with the account of eqs 35 and 36

$$\omega\Psi(R) + h^2 = k \quad (37)$$

Equation 37, above, provides the relationship between the three unknown variables h, k, and $\Psi(R)$. To find an additional relationship between these variables we integrate eq 36 and represent the electrostatic potential Ψ_3 in the following form:

$$\int_{\Psi_3(x)}^0 \frac{d\Psi}{\sqrt{\omega\Psi + ke^{\Psi} + h^2 - k}} = 2(x - H)/H_0 \quad (38)$$

By substituting $x = R$ in eq 38, we arrive at the third equation, which links the unknown variables k, h and $\Psi(R)$. Namely

$$\int_{\Psi(R)}^0 \frac{d\Psi}{\sqrt{\omega\Psi + ke^{\Psi} + h^2 - k}} = 2(d - h) \quad (39)$$

The expressions in eqs 34, 37, and 39 constitute a set of the three equations that determine the three unknown variables, k, h, and $\Psi(R)$ at given values of r, ζ, and ω (or equivalently, $\gamma = \omega r/\zeta$). This set of equations can be solved analytically for the particular case, $\gamma = 1$, i.e., when all the counterions are immobilized in the sublayer.

3.2.1. Completely Immobilized Opposite Charge, $\gamma = 1$. When $\gamma = 1$, we have $\omega = \zeta/r$ while the value of k equals zero (since $\rho(H) = 0$). Correspondingly, eq 34 gives for the brush thickness

$$h = \frac{r}{(1 + r/\zeta)} \quad (40)$$

while eq 37 determines the value of $\Psi(R)$ as

$$\Psi(R) = -\frac{r\zeta}{(1 + \zeta/r)^2} \quad (41)$$

By solving eq 38 for $k = 0$, we obtain the electrostatic potential Ψ_3. That is

$$\Psi_3(\xi) = \frac{\zeta}{r}\left[\xi - \frac{r}{(1 + r/\zeta)}\right]\left[\xi - r\frac{(1 + 2r/\zeta)}{(1 + r/\zeta)}\right] \quad h < \xi < r \quad (42)$$

We recollect that inside the brush (i.e., at $\xi < h$), the shape of the electrostatic potential remains parabolic, and Ψ_1 is given by eq 5. In the range $\xi > r$, the electrostatic potential is constant since there is no charge outside the sublayer. As a result, we have

$$\Psi_2(\xi) = \Psi(R) \quad (43)$$

where $\Psi(R)$ is determined by eq 41. The profile of polymer units becomes a step function

$$c(\xi)/c_0 = 1/h = 1/r + 1/\zeta \quad (44)$$

while the distribution function of the free ends yields

$$g(\xi)H_0 = \frac{\xi}{h\sqrt{h^2 - \xi^2}} \quad (45)$$

We note that a steplike profile of polymer was also found when all the counterions were immobilized at a fixed distance $x = D > H$ from the grafting surface.[13] Though the thickness of the brush is different for the two cases, the shape of the profile remains the same (i.e., steplike).

3.2.2. Partially Immobilized Charge, $\gamma < 1$. At an arbitrary value of γ, a solution of the set of eqs 34, 37, and 39 can be obtained numerically. Provided that solution of this set is available, we can obtain the final results for the polymer profile (eq 33), the profiles of ions in all the three regions and the distribution function of the free ends $g(x)$. Namely, the polymer profile is given by

$$c(\xi)/c_0 = \frac{\gamma}{r} + \zeta^{-1} + k\zeta^{-1}e^{h^2-\xi^2} \quad (46)$$

The distributions of the ions read

$$\rho_1(\xi)/\rho_0 = k\zeta^{-1}e^{h^2-\xi^2} \quad \xi < h \tag{47}$$

$$\rho_3(\xi)/\rho_0 = k\zeta^{-1}e^{\Psi_3(\xi)} \quad h < \xi < r \tag{48}$$

where Ψ_3 is determined by eq 38, and

$$\rho_2(\xi)/\rho_0 = \frac{\zeta^{-1}}{\left[t - r + \frac{1}{\sqrt{k}}e^{-\Psi(R)/2}\right]^2} \quad \xi > r \tag{49}$$

As for the distribution of the free ends, we obtain from eqs 45 and 27

$$g(\xi)H_0 = \xi\zeta^{-1}\left[\frac{\gamma\zeta/r + 1 + k}{\sqrt{h^2 - \xi^2}} + 2ke^{h^2-\xi^2}\int_0^{\sqrt{h^2-\xi^2}} e^{-t^2}\,dt\right] \tag{50}$$

Below we discuss the effect of the total value of the sublayer charge and of the form of its distribution on the structure of the brush in more detail.

4. Results

We start with one of the major characteristics of the brush, its thickness H.

4.1. Thickness of the Polyelectrolyte Brush. The overall brush thickness H (or equivalently, the reduced overall thickness, $h = H/H_0$) determines the width of the spatial region where the tethered polyions distribute their units. The free, ungrafted ends of the chains are also distributed in this range. When the presurface layer is not charged, i.e., $\gamma = 0$, the thickness h of the brush is given by eq 23 at $\gamma = 0$. Namely, h is the root of the equation

$$\zeta = h + h^2e^{h^2}\int_0^h e^{-t^2}\,dt \tag{51}$$

We denote the solution of this equation as $h(0)$. Depending on the value of $\zeta = H_0/\Lambda$, one finds two different asymptotics for $h(0)$. At $\zeta \to 0$, we have $h \approx \zeta$, while at $\zeta \to \infty$, h diverges logarithmically (see ref 14 for more details).

Charging of the sublayer (i.e. an increase in γ) affects the brush thickness h in a specific manner. If the thickness of the sublayer, $r = R/H_0$ is smaller than $h(0)$, then charging of the sublayer causes contraction of the brush, i.e., a decrease in h according to eq 23. At a certain value of $\gamma = \gamma^*$, the brush thickness becomes equal to the thickness of the sublayer, i.e., $h(\gamma^*) = r$. At $\gamma > \gamma^*$, the brush is totally absorbed into the sublayer and $h < r$. Here, the brush thickness, $h(\gamma)$ is determined by eqs 34, 37, and 39. Finally, at $\gamma = 1$, h reaches its limiting value, $h = h(1)$, as determined by eq 40.

If the thickness of the sublayer r is high enough, so that $r > h(0)$, the behavior of the system becomes more complicated. Here, h is determined by eqs 34, 37, and 39 for all values of γ. Depending on the particular value of r, one can find two different situations. Namely, $h(1) > h(0)$ and $h(1) < h(0)$. In the former case, the brush thickness increases monotonically with increases in γ. In the latter case, i.e., when $h(1) < h(0) < r$, the dependence $h = h(\gamma)$ exhibits a maximum.

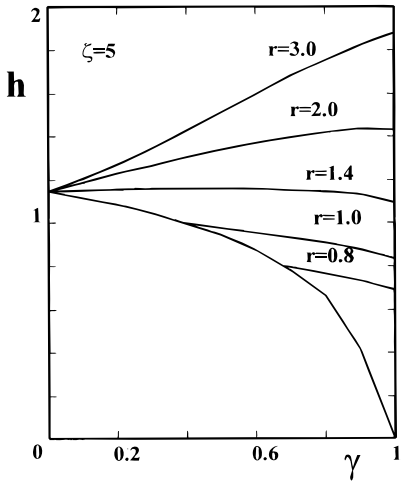

Figure 2. Overall reduced brush thickness $h = H/H_0$ vs γ at various values of sublayer thickness $r = R/H_0$ (indicated). $\zeta = H_0/\Lambda = 5$.

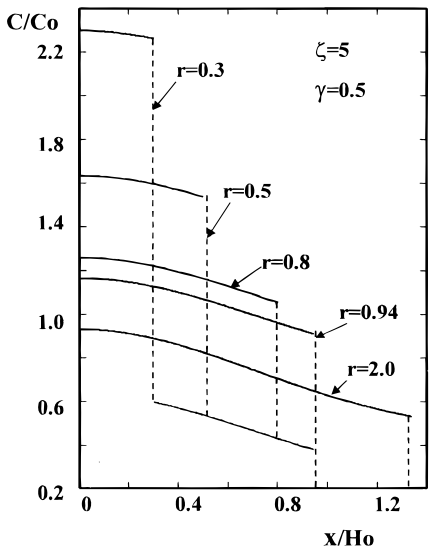

Figure 3. Reduced polymer concentration c/c_0 vs reduced distance $\xi = x/H_0$ at various values of sublayer thickness $r = R/H_0$ (indicated). Here, $\gamma = 0.5$ and $\zeta = 5$. For $r = 2$ (thick layer, $r > h$), the brush is totally absorbed into the sublayer. At $r = 0.94$, $h = r$. For $r = 0.8$, 0.5, and 0.3 (thin layers), the brush is absorbed partially. Its thickness $h = 0.94$ stays constant, while polymer profiles exhibit a jump at $\xi = r$.

Figure 2 demonstrates the dependences of the brush thickness h vs γ at various values of r calculated according to eqs 23, 34, 38, and 40. When $r < h(0)$, an initial decrease in h does not depend on a particular value of r, and h follows the master curve determined by eq 23. Only when γ reaches the critical value, $\gamma^*(r)$, does the dependence $h(\gamma)$ change, and h decreases more slowly than predicted by eq 23. The value of γ^* is calculated by substituting $h = r$ into eq 23. When $r > h(0)$, we find a monotonic increase in h for relatively high values of r and a curve with a maximum when r is comparable to $h(1)$. We recollect that those dependences for h are found for a brush, which is already totally embedded into the sublayer at $\gamma = 0$.

4.2. Polymer Profile. Figures 3 and 4 demonstrate the profiles of polymer units as function of the reduced distance $\xi = x/H_0$. Those profiles were calculated for a

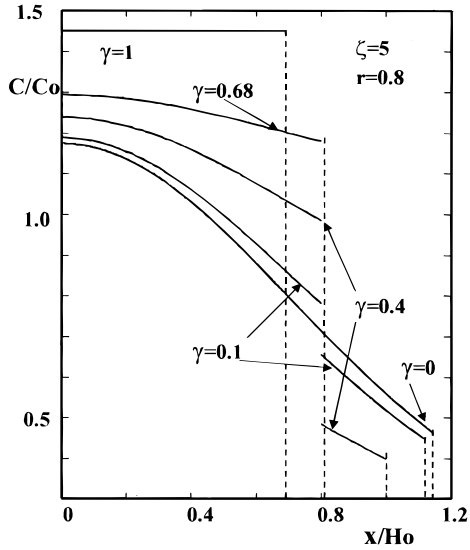

Figure 4. Reduced polymer concentration c/c_0 vs reduced distance $\xi = x/H_0$ at various values of γ. Here, the sublayer thickness is fixed, $r = 0.8$, and $\zeta = 5$. At $\gamma = 0$, the sublayer is embedded into the brush. At $\gamma = 0.1$ and $\gamma = 0.4$, the brush is partially absorbed and polymer profiles exhibit a jump at the edge of sublayer, $\xi = r = 0.8$. At $\gamma = 0.68$, the brush is absorbed totally, $h = r$. At $\gamma = 1$, the polymer profile becomes steplike.

uniformly charged sublayer ($\rho_s(x) = \rho_s$) according to eqs 23 and 33 as

$$c(\xi)/c_0 = \frac{\gamma}{r} + \zeta^{-1} + k\zeta^{-1}e^{h^2-\xi^2} \quad \xi < r \qquad (52)$$

and

$$c(\xi)/c_0 = \zeta^{-1} + h^2\zeta^{-1}e^{h^2-\xi^2} \quad r < \xi < h \qquad (53)$$

where $c_0 = Na^3/sH_0$ is the characteristic concentration of polymer units, while the values of h and k were determined from eqs 21 and 23 for $r < h$ and eqs 34, 37, and 39 for $r > h$.

Figure 3 presents the profiles for a fixed value of charge in the sublayer γ (=0.5) and different values of the layer width r, whereas Figure 4 demonstrates the variation in the profiles with increases in γ at a fixed value of r. These results indicate that when $r > h$, the polymer profiles are smooth functions in the whole range $\xi < h$ and exhibit a jump only at the outer edge, $\xi = h$. The shape of the profile changes, however, dramatically when $r < h$. Here, the polymer profile exhibits an additional jump at the boundary $\xi = r$ inside the brush. Decreases in r makes this jump more pronounced and, as a result, the profile becomes more inhomogeneous (see Figure 3).

Increases in γ (at a fixed value of r) lead to a compactization of the profile. As seen from Figure 4, at $\gamma = 0$, the profile is extended and smooth at $\xi < h$. As γ is increased, the polymer units start to concentrate in the sublayer and the profile shrinks. Here, we find a denser part of the profile at $\xi < r$ and a looser tail at $\xi > r$. When γ reaches a critical value, $\gamma = \gamma^*$, the loose tail disappears, and the profile becomes rather compact and homogeneous. Further increases in γ lead to further compactization of the brush, and at $\gamma = 1$, the profile acquires a steplike shape.

4.3. Distribution of the Free Ends. The distribution of the free ends of the tethered polyions, $g(x)$, reflects the shape of the polymer profile, $c(x)$. (The interconnection between the two functions is provided by eq 27). Appearance of jumps in the polymer profile results in discontinuities in the profile of the free ends. Figures 5 and 6 demonstrate the distributions of the free ends, $g(\xi)$, corresponding to the polymer profiles in Figures 3 and 4. Those dependences were calculated according to eqs 28 and 45. As seen from Figures 5 and 6, the profile of the free ends of the tethered polyions can be rather spectacular, particularly when $h > r$. Due to appearance of the jumps in the polymer profiles, the distribution of the free ends becomes essentially nonmonotonic. It passes through a maximum (diverges) at $\xi = r$ and then passes through a second maximum at the edge of the brush, $\xi = h$. The areas under the curves for $\xi < r$ and $\xi > r$ determine the fractions of chains in the sublayer and the outer part of the brush, respec-

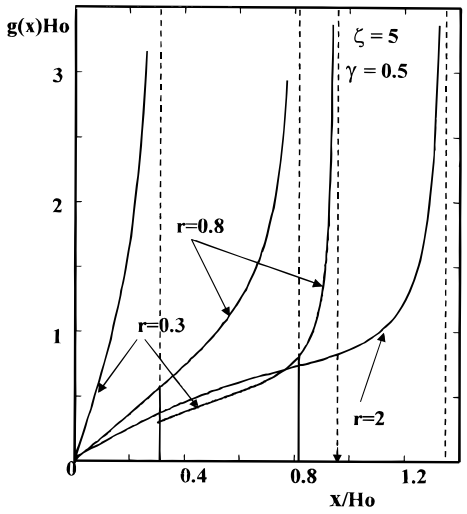

Figure 5. Distribution function of the free ends, $g(\xi)H_0$, vs reduced distance $\xi = x/H_0$ at various values of sublayer thickness r (indicated). Here, $\gamma = 0.5$ and $\zeta = 5$. At $r = 2$, the brush is embedded into the sublayer, and $g(x)$ diverges only at the outer edge of the brush (indicated by dashed line). At $r = 0.8$, the brush is absorbed partially and $g(x)$ exhibits a divergence at $\xi = h$ (dashed line with an arrow) and a divergence at $\xi = r$ (indicated by dashed/solid line positioned at $\xi = 0.8$). At $r = 0.3$, $g(\xi)$ diverges at $\xi = h$ (dashed line with an arrow) and at $\xi = r$ (dashed/solid line positioned at $\xi = 0.3$).

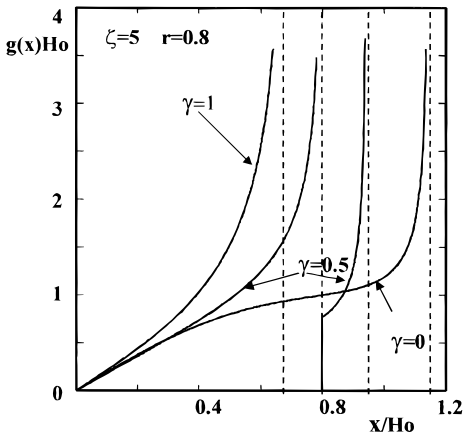

Figure 6. Distribution function of the free ends $g(\xi)H_0$ vs reduced distance $\xi = x/H_0$ at various values of γ (indicated). Here, $r = 0.8$ and $\zeta = 5$. At $\gamma = 0$, $g(\xi)$ diverges only at the edge of the brush. At $\gamma = 0.5$, the brush is partially absorbed into the sublayer, and $g(\xi)$ diverges at $\xi = h$ and $\xi = r$. At $\gamma = 1$, the brush is absorbed totally, and $g(x)$ diverges only at the outer edge of the brush, $\xi = h$.

tively. The general shape of the profiles indicates the internal "segregation" of chains in the brush due to the charged sublayer. With increases in γ, the larger part of the chains is localized inside the sublayer and less chains form the looser, external part of the brush. When all the chains are "condensed" into the sublayer and $h < r$, the distribution of the free ends becomes more "homogeneous". That is, $g(x)$ monotonically increases to the periphery of the brush and diverges only at its outer edge, $\xi = h$.

4.4. Absorbed Amount and Fraction of Absorbed Polyions. To get more insight into the properties of our system, we introduce the additional characteristics. Namely, an "absorbed amount" of polymer, Θ, defined as

$$\Theta = \frac{s}{N}\int_0^R c(x)\,\mathrm{d}x \tag{54}$$

and the fraction of absorbed polyions

$$\Gamma = \int_0^R g(x)\,\mathrm{d}x \tag{55}$$

The former parameter, Θ, determines a fraction of polymer units inside the charged sublayer, while the latter one, Γ gives a fraction of the polyions which are totally embedded into the sublayer. By substituting the corresponding eqs 52 and 53 for the polymer profile and the distribution of the free ends (eq 28) into eqs 55 and 54, we arrive at the following expressions

$$\Theta = \zeta(r + h^2\mathrm{e}^{h^2}\int_0^r \mathrm{e}^{-t^2}\,\mathrm{d}t) + \gamma \tag{56}$$

and

$$\Gamma = (1 + h^2)\zeta^{-1}\left(h - \sqrt{h^2 - r^2} + \frac{h^2}{2}\int_0^{r^2}\mathrm{e}^{h^2-t'}\,\mathrm{d}t'\int_0^{\sqrt{h^2-t'}}\mathrm{e}^{-t^2}\,\mathrm{d}t\right) + \gamma \tag{57}$$

As follows from the above equations, at any value of $r > 0$, both $\Theta > \gamma$ and $\Gamma > \gamma$. However, decreases in r lead to the corresponding decreases in Θ and Γ. In the limit $r \to 0$, we find $\Theta = \gamma$ and $\Gamma = \gamma$. In other words, when the thickness of the sublayer R becomes negligibly small with respect to the characteristic length scale H_0, a fraction γ of all the polyions are transferred from the brush into the sublayer. As a result, one can envision the system as a polyelectrolyte brush tethered onto a noncharged surface with an effective grafting density, $s_{\mathrm{eff}}^{-1} = s^{-1}(1 - \gamma)$.

4.5. Free Energy of Polyelectrolyte Brush. We finish this section with calculating the free energy of the brush ΔF at an arbitrary value of γ. W focus at the case of partial absorption (that is, $h > r$). As discussed in ref 14, the free energy of our system consists of the three contributions

$$\Delta F = \Delta F_{\mathrm{pol}} + \Delta W - T\Delta S_{\mathrm{ions}} \tag{58}$$

The first contribution, ΔF_{pol}, incorporates the conformational losses of the polyions due to the stretching normally to the surface. Under the conditions of a strong stretching limit, ΔF_{pol} is given by[24]

$$\Delta F_{\mathrm{pol}}/k_{\mathrm{B}}T = \frac{3}{2a^2}\int_0^H g(x')\,\mathrm{d}x'\int_0^{x'} E(x,x')\,\mathrm{d}x \tag{59}$$

where

$$E(x,x') = \frac{\mathrm{d}x}{\mathrm{d}n} = \frac{\pi}{2N}\sqrt{x'^2 - x^2} \tag{60}$$

is the function of the local stretching of the chain. Expression 59 can be rewritten with the account of eq 27 as

$$\Delta F_{\mathrm{pol}}/k_{\mathrm{B}}T = \frac{3\pi^2 s}{8a^2N^2}\int_0^H \mathrm{d}x\int_x^H x'c(x')\,\mathrm{d}x' \tag{61}$$

After substituting expressions 51 and 52 for the polymer profile into eq 61 and calculating the integrals, we have

$$\Delta F_{\mathrm{pol}}/k_{\mathrm{B}}T = \alpha N\left[\gamma r^2 + \frac{(1-\gamma)}{2} - \frac{h}{2\zeta} - \frac{h^3}{6\zeta}\right] \tag{62}$$

The electrostatic contribution ΔW accounts for the electrostatic energy due to the spatial distribution of charges in the system. It yields

$$\Delta W/k_{\mathrm{B}}T = \frac{\epsilon s}{8\pi k_{\mathrm{B}}T}\int_0^\infty (\nabla\psi)^2\,\mathrm{d}x \tag{63}$$

where $\psi(x)$ is the electrostatic potential and $-\nabla\psi(x)$ is the strength of the electric field. By substituting the corresponding electrostatic potentials, eqs 5 and 22, into the above expression and performing the integration, we obtain

$$\Delta W/k_{\mathrm{B}}T = \alpha N\left[\frac{h^3}{3\zeta} + \frac{h}{\zeta}\right] \tag{64}$$

Finally, the entropic contribution, ΔS_{ions}, is determined by the translational entropy of the mobile ions

$$\Delta S_{\mathrm{ions}}/k_{\mathrm{B}} = s\int_0^\infty \rho(x)\ln[\rho(x)]\,\mathrm{d}x \tag{65}$$

By substituting the corresponding expressions for the ion distribution inside and outside of the brush, eqs 24 and 25, we arrive after some algebra at the following expression for ΔS_{ions}

$$\Delta S_{\mathrm{ions}}/k_{\mathrm{B}} = \alpha N\left[(1-\gamma)\ln\left(\frac{\rho_o h^2\mathrm{e}^{h^2}}{\zeta}\right) - \frac{(1-\gamma)}{2} - \frac{3h}{2\zeta} - \frac{h^3}{2\zeta}\right] \tag{66}$$

The total free energy of the system (per area s) thus yields

$$\Delta F/k_{\mathrm{B}}T = \alpha N\left[(1-\gamma)\ln\left(\frac{\rho_0 h^2\mathrm{e}^{h^2}}{\zeta}\right) + \gamma r^2 - \frac{h}{\zeta} - \frac{h^3}{3\zeta}\right] \tag{67}$$

where h is determined by eq 23.

Figure 7 shows the dependences of all the three components, ΔF_{pol}, ΔW, ΔS_{ions}, and the total free energy, ΔF, vs the sublayer charge, γ.

5. Discussion

In our earlier work[26] we considered the effect of the oppositely charged surface on the conformations of sparsely grafted polyions. We have demonstrated that the Coulomb attraction between polyions and the surface results in the adsorption of the charged chains (i.e.

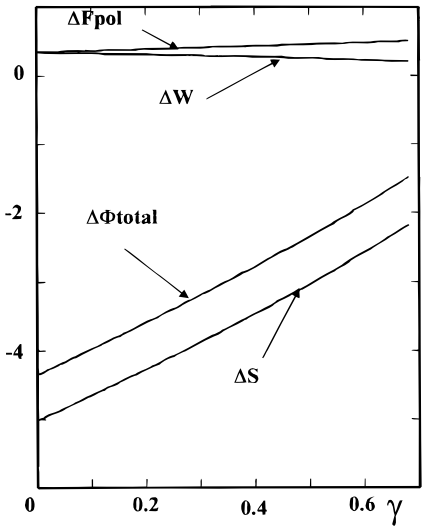

Figure 7. Various contributions to the free energy, ΔF_{pol}, ΔW, ΔS, and total free energy, $\Delta\Phi_{total}$, vs amount of charge in sublayer γ.

in their confinement in the presurface region) even at relatively low surface charge density. The present paper deals with another limit. That is, the polyions are grafted rather densely so that the interchain Coulomb repulsions become essential. The chains conformations are determined now by the competition between the interchain repulsion and the attraction to the oppositely charged sublayer.

Our results demonstrate that the interaction of a polyelectrolyte brush with an oppositely charged sublayer can dramatically affect the brush structure. Namely, when the sublayer is relatively thin ($r = R/H_0 \ll 1$), the tethered polyions shield an opposite charge by delegating a certain part of the chains into the sublayer. This redistribution of polymer manifests itself in various characteristics of the brush. Namely, the polymer profile becomes more "inhomogeneous" due to the accumulation of monomer units in the sublayer at the cost of making more loose a distal part of the brush. The distribution of the free ends indicates an increased fraction of the chains totally localized in the sublayer.

A spectacular feature of these rearrangements is that due to the interaction with the sublayer, the brush becomes essentially heterogeneous. One can envision the system as undergoing an internal segregation which is particularly noticeable when $r \to 0$. Under these conditions, the fraction γ of all the chains are totally "absorbed" into the sublayer, whereas the rest of the chains still form a brush. The absorbed polyions shield the charge of the sublayer. Their disappearance from the body of the brush effectively changes the grafting density of the remaining chains. As a result, we can envision a partially absorbed polyelectrolyte brush as a nonabsorbing system of the chains with an effective grafting density $s_{eff}^{-1} = s^{-1}(1 - \gamma)$. Such structure of the brush turns out to be more favorable than partial delegating of the units into the sublayer by each tethered polyion.

We note, however, that in our model both, the absorbed and nonabsorbed polyions are stretched with respect to the Gaussian size ($aN^{1/2}$). Thus, a limit $r \ll 1$ implies that the thickness of the sublayer R is still sufficiently high to satisfy the inequality $aN^{1/2} \ll R \ll H_0 \simeq a\alpha^{1/2}N$.

We can employ a simple scaling argument to justify the scenario of internal segregation. Consider a polyelectrolyte brush with the grafting area s under the conditions $\zeta = H_0/\Lambda \gg 1$. In this range of ζ corresponding to the so-called "osmotic" regime,[1,2] the counterions are condensed in the brush and screen the interactions between the polyions. The average brush thickness scales here as $H \simeq H_0 \simeq \alpha^{1/2}Na$. The free energy of the system is determined by the translational entropy of the ions to give

$$\Delta F/k_BT \simeq \frac{\alpha N}{s}\ln\left(\frac{\alpha N a^3}{sH_0}\right) \simeq \frac{\alpha N}{s}\ln\frac{\alpha^{1/2}a^2}{s} \qquad (68)$$

per unit area. Localization of part γ of all the counterions on the surface creates the surface charge and increases the free energy of the system. Neutralization of this charge can be attained by either delegating the fraction γ of all the chains onto the surface (that is, by the segregation of the polyions) or by partial absorption of each chain (that is, by delegating to the surface the fraction γ of units by each chain). In the first case, we renormalize the grafting area per chain as $s' = s/(1 - \gamma)$, while in the second case, we effectively change the length of the tethered polyions as $N' = N(1 - \gamma)$. (A segment of $(N - N')$ units compensates the excess charge per chain on the surface). By substituting the values of s' and N' into expression 68 for the free energy, we find that $\Delta F_1 - \Delta F_2 = \ln(1 - \gamma) < 0$. Thus, the internal segregation of the polyions into "absorbed " and "nonabsorbed" chains is more favorable than the partial absorption of each polyion. Since the segregation scenario works for the osmotic regime of a polyelectrolyte brush, where the electrostatic interactions are screened at most, it should be also valid for weaker screening, i.e., at an arbitrary value of ζ.

We note that the effect of segregation of the tethered chains was reported earlier by Marko et al.[27] Those authors considered a neutral polymer brush exposed to external fields. The findings of that work indicated that an attractive external field causes a segregation of the tethered chains into the two classes (i.e., "absorbed" and "nonabsorbed" chains). The chemical potential of the polymer units retains its parabolic shape, and the free ends of the chains are distributed throughout the brush. The effect of an attractive force can be accounted for by renormalizing the grafting area per chain, so that the brush thickness H diminishes. A repulsive external field leads to an increase in the brush height H. However, an additional stretching of the brush gives rise to a dead zone (a zone without the free ends) near the grafting surface, and the chemical potential is not parabolic anymore.

The results of our work demonstrate that for partially absorbed polyelectrolyte brushes ($H > R$), the decreases in H can be indeed accounted for by a renormalization of the grafting area s as $s' = s/(1 - \gamma)$. However, in totally absorbed brushes ($H < R$), the behavior of the system is more complex. Namely, we can find both a decrease and an increase in H with increases in γ. The latter trend is found when the brush is embedded into a thick sublayer; see Figure 2. The effect is most pronounced when $\gamma = 1$, i.e., when all the counterions are immobilized. Now, the attraction between the oppositely charged brush and sublayer pushes the chains to stretch additionally (in comparison with the unperturbed system, $\gamma = 0$). In effect, the tethered

chains are subjected to a "repulsive" potential. However, this stretching of the brush due to the interaction with the sublayer does not lead to the appearance of the dead zones; i.e., the free ends of the tethered polyions are distributed throughout the range $0 < x < H$. The brush height is determined by eq 40, the profile of polymer units becomes steplike, eq 44, while the free ends concentrate at the edge of the brush according to eq 45.

Our findings indicate that in partially absorbed polyelectrolyte brushes ($h > r$), the overall brush thickness h does not depend on the particular form of the charge distribution in the sublayer. According to eq 23, only the total amount of the immobilized charge (or, equivalently the value of γ) counts. As a result, simple renormalization of the grafting area as $s \rightarrow s/(1 - \gamma)$ accounts for variation in h at various distributions of charge in the sublayer.

Since the electrostatic potential inside the brush remains parabolic and is affected only through the value of h, the distributions of the mobile ions inside and outside the brush (that are determined by eqs 24 and 25 are also not sensitive to the particular form of $\rho_s(x)$.

However, the profile of polymer units, $c(x)$, reproduces the charge distribution in the layer, $\rho_s(x)$, with an additional shift due to the mobile counterions according to eq 26.

The only restriction on the shape of the charge distribution $\rho_s(x)$ is imposed by the condition that the distribution function of the free ends, $g(x)$, which is related to the polymer profile through eq 27, remains positive in the whole range $0 < x < H$. For the charge distributions $\rho_s(x)$, which are characterized by a negative or zero values of the derivative, $(d\rho_s(x)/dx) < 0$, $g(x)$ remains positive throughout the brush. We note that such type of charge distribution is typical for layers of adsorbed or tethered polyelectrolytes at solid−liquid interfaces that can mimic a charged sublayer of our system. When the sign of the derivative,$(d\rho_s(x)/dx)$, changes, the distribution function of the free ends, $g(x)$, can still be positive inside the brush. For such charge distributions, the behavior of $g(x)$ should be checked for any particular shape of $\rho_s(x)$. For totally absorbed systems (i.e., when $H < R$), the situation is more delicate. Here, the value of the brush thickness, h, depends not only on the total amount of the immobilized charge in the layer (or γ), but also on the value of k (eq 34), which, in turn, is determined by the charge distribution in the layer through the Poisson−Boltzmann equation. Thus, we do not find here the same "degree of universality" as for partially absorbed systems. Finally, we emphasize that the results of this paper were obtained for a salt-free case, i.e., where no salt ions are added into solution and the electrostatic interactions between the polyions are screened only by the counterions. In our forthcoming paper,[28] we shall focus on the salt-added solution and investigate the effect of the salt ions on the absorption of a polyelectrolyte brush.

Acknowledgment. We are thankful to F. Leermakers for helpful remarks on the manuscript. O.V.B. appreciates the hospitality of Prof. G. J. Fleer and Prof. M. A. Cohen Stuart in the University of Wageningen and the NWO research grant. E.B.Z. acknowledges the hospitality of Prof. A. C. Balazs at the University of Pittsburgh. This work was partially supported by a NWO Dutch−Russian program for agricultural and food research and a TAPPI research grant.

References and Notes

(1) Pincus, P. *Macromolecules* **1991**, *24*, 2912. Ross, R.; Pincus, P. *Macromolecules* **1992**, *25*, 1503.
(2) Borisov, O. V.; Birshtein, T. M.; Zhulina, E. B. *J. Phys. II* **1991**, *1*, 521. Zhulina, E. B.; Borisov, O. V.; Birshtein, T. M. *J. Phys. II* **1992**, *2*, 63. Borisov, O. V.; Zhulina, E. B.; Birshtein, T. M. *Macromolecules* **1994**, *27*, 4795. Zhulina, E. B.; Birshtein, T. M.; Borisov, O. V. *Macromolecules* **1995**, *28*, 1491.
(3) Miklavic, S. J.; Marcelja, S. *J. Phys. Chem.* **1988**, *92*, 6718.
(4) Misra, S.; Varanasi, S.; Varanasi, P. P. *Macromolecules* **1989**, *22*, 4173.
(5) Misra, S.; Varanasi, S. *J. Chem. Phys.* **1991**, *95*, 2183.
(6) Misra, S.; Mattice, W. L.; Napper, D. H. *Macromolecules* **1994**, *27*, 7090.
(7) Wittmer, J.; Joanny, J.-F. *Macromolecules* **1993**, *26*, 2691.
(8) von Goeler, F.; Mathukumar, M. *Macromolecules* **1995**, 28, 6608; *J. Chem. Phys.* **1996**, *105*, 11335.
(9) Dan N.; Tirrel M. *Macromolecules* **1993**, *26*, 4310.
(10) Israels, R.; Leermakers, F. A. M.; Fleer, G. J.; Zhulina, E. B. *Macromolecules* **1994**, *27*, 3249.
(11) Israels, R,; Leermakers, F. A. M.; Fleer, G. J. *Macromolecules* **1994**, *27*, 3087.
(12) Lyatskaya, Yu. V,; Leermakers, F. A. M.; Fleer, G. J.; Zhulina, E. B.; Birshtein, T. M. *Macromolecules* **1995**, *28*, 3562.
(13) Borisov, O. V.; Zhulina, E. B. *J. Phys. II* **1997**, *7*, 449.
(14) Zhulina, E. B.; Borisov O. V. *J. Chem. Phys.* **1997**, *107*, 5952.
(15) Mir, Y.; Auroy, P.; Auvray, L. *Phys. Rev. Lett.* **1995**, *75*, 2863.
(16) Watanabe, H.; Patel, S. S.; Argillier, J. F.; Parsonage, E. E.; Mays, J.; Dan-Brandon, N.; Tirrell, *M. Mater. Res. Soc. Symp. Proc.* **1992**, *249*, 255.
(17) Tirrell, M. In *Solvents and Self-Organization of Polymers*; Webber, S. E., Munk, P., Tuzar, Z., Eds.; NATO ASI Series E: Applied Sciences-327; Kluwer Academic Publishers: Dordrecht, The Netherlands, 1996; p 281.
(18) Schorr, P.; Tirrell, M. Manuscript in preparation.
(19) Napper D. H. *Polymeric Stabilization of Colloidal Dispersions*; Academic Press: London, 1985.
(20) *Stealth Liposomes*, Lasic, D., Martin, F., Eds.; CRC Press: Boca Raton, FL, London, Tokyo, 1995.
(21) Mammen, M.; Choi, S.-K.; Whitesides, G. Manuscript in preparation.
(22) Fleer, G. J.; Cohen Stuart, M. A.; Scheutjens, J. M. H. M.; Cosgrove, T.; Vincent, B. *Polymers at Interfaces*; Chapman & Hall: London, 1993.
(23) Barrat, J.-L.; Joanny, J.-F. *Europhys. Lett.* **1993**, *24*, 333.
(24) Semenov, A. N. *Sov. Phys. JETP* **1985**, *61*, 733.
(25) Israelachvili J. N. *Intermolecular and Surface Forces*, Academic Press: London, 1985.
(26) Borisov O. V.; Birshtein T. M.; Zhulina E. B. *J. Phys. II* **1994**, *4*, 913.
(27) Marko, J. F.; Johner, A.; Marques, C. M. *J. Chem. Phys.* **1993**, *99*, 8142.
(28) Zhulina, E. B.; Borisov, O. V.; Leermakers, F. A. M. Manuscript in preparation.

MA980845J